ELSEVIER

S0032-3861(96)00409-0

Polymer Vol. 37 No. 25, pp. 5559–5568, 1996

0032-3861/96/$15.00+0.00

Application of small-angle neutron scattering to the study of the structure of starch granules

Paul J. Jenkins and Athene M. Donald*
Cavendish Laboratory, Madingley Road, Cambridge, CB3 0HE, UK
(Received 29 September 1995; revised 23 January 1996)

The use of contrast variation to provide detailed information on local composition from small-angle neutron scattering (SANS) is a well established technique for synthetic polymers. However, it has been much less exploited in the field of biopolymers. In this present paper the approach is described in its application to understanding the distribution of water within waxy maize starch granules. On the basis of small-angle X-ray scattering, starch granules have been modelled as containing three regions, namely semicrystalline stacks containing alternating crystalline and amorphous lamellae, which are embedded in a matrix of amorphous material. By using the results obtained from SANS studies of starch dispersed in water with different D_2O contents it has been possible to quantify for the first time, the water contents in each of these three regions.

(Keywords: starch; small-angle neutron scattering; water content)

INTRODUCTION

Starch is laid down in the form of granules that function as an energy reserve. These granules vary in size and shape with botanic origin, but in each case an examination of these granules under optical or electron microscopy reveals pronounced concentric rings[1]. The fact that these rings are alternately of semicrystalline and amorphous composition is shown by their differing susceptibility to α-amylase attack. They are known as 'growth rings'. At a higher level of organization, both scattering studies[2–4] and electron microscopy[5–8] have shown the semicrystalline rings to be composed of stacks of alternating crystalline and amorphous lamellae. These stacks give rise to the marked peak that is observed in small-angle X-ray and neutron scattering experiments.

The starch granule contains two main components, the polysaccharides amylose and amylopectin. Amylopectin is a highly branched molecule. Nevertheless, the evidence is that the crystallinity is associated with this component of the starch granule: starches such as waxy maize, which contain no amylose, exhibit comparable crystallinity to normal starches with amylose contents of $\sim 30\%$. The currently accepted crystalline structure consists of a radial arrangement of clusters of amylopectin. This structure was proposed originally by Robin *et al.*[9,10]. Each cluster contains a region which is high in branch points (the amorphous lamella) and a region where short chain segments of amylopectin have formed double helices (the crystalline lamella).

Building on the two separate pieces of evidence of growth rings and semicrystalline lamellae, Cameron and Donald[4] developed a model which allows quantification of the various parameters needed to describe this complex structure. The starch granule structure is modelled as a finite number of lamellae of alternating electron density (crystalline regions C with high electron density ρ_c, and amorphous regions A with low, ρ_a), embedded in a background region (B) of a third electron density ρ_b, which is assumed to correspond to the amorphous growth ring (*Figure 1*). Crudely, the growth rings, being comparatively large structures, give rise to scattering at small q, whereas the main interface peak arises from the semicrystalline lamellae. The small-angle X-ray scattering has been quantitatively predicted for such a model[12] and can be fitted to the experimental scattering data. The scattering intensity $I_1(q)$ is given by the following:

$$I_1(q) = \frac{2(\Delta\rho)^2)}{q^2}\mathrm{Re}\left[\frac{(1-F_c)(1-F_a)}{(1-F_cF_a)} + \frac{1}{N}F_a\frac{(1-F_c)^2}{(1-F_cF_a)^2}(1-(F_cF_a)^N)\right] + \frac{2(\Delta\rho)^2)}{q^2N}\mathrm{Re}\left[\frac{(\Delta\rho_u)^2}{(\Delta\rho)^2}(1-(F_cF_a)^N) - \frac{\Delta\rho_u}{\Delta\rho}(1+F_a)\frac{(1-F_c)}{(1-F_cF_a)}(1-(F_cF_a)^N)\right] \quad (1)$$

where F_c and F_a are the Fourier transforms of the crystalline and amorphous distribution functions, respectively. In the above equations:

$$\Delta\rho = \rho_c - \rho_a \quad (2)$$

and

$$\Delta\rho_u = \rho_a - \rho_b \quad (3)$$

and N is the total number of lamellae in a stack. The total

*To whom correspondence should be addressed

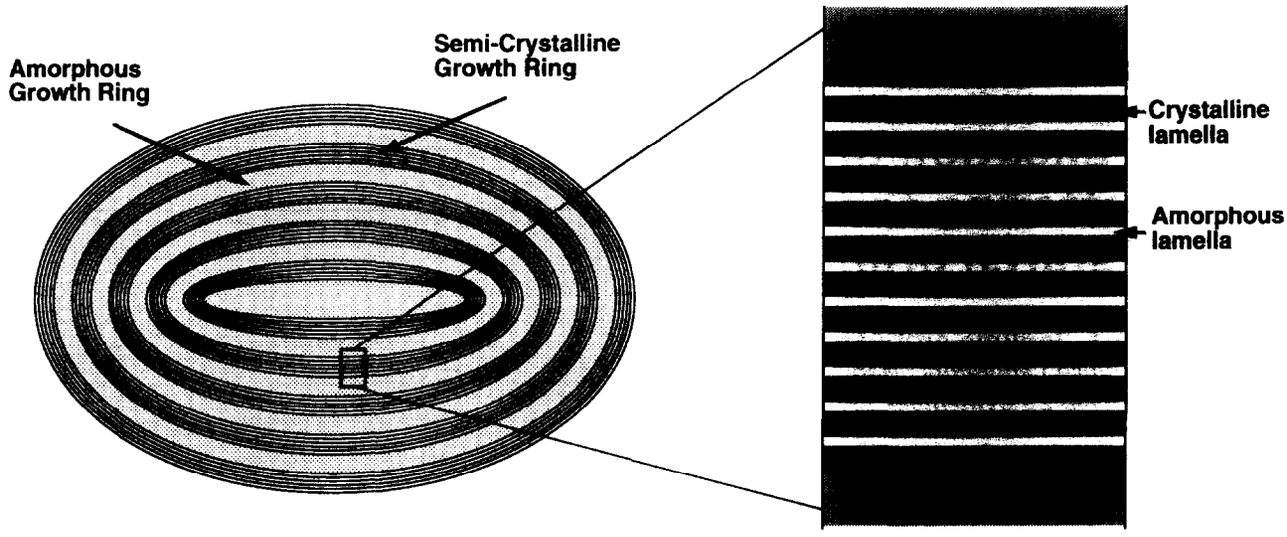

Figure 1 Model for analysing small-angle scattering of the starch granule (after ref. 11)

scattering then needs to be corrected by the Lorentz correction, in order to allow for the random distribution of the stacks.

Implicit in this analysis, as well as the three electron densities referred to above, are parameters describing the overall repeat distance (amorphous plus crystalline lamellae), the percentage of crystalline material within the semicrystalline stack, and the distribution of lamellar sizes. All fitting parameters are varied concurrently until the best correlation is achieved between the experimental data and predicted scattering. A more complete description of the lamellar stack model (which is a variant on the simple black-and-white model of Hosemann[13]) and its applicability to the starch granule is given by Cameron and Donald[4,14].

In the model proposed so far on the basis of small-angle X-ray scattering (SAXS), only the relative electron densities could be obtained, as absolute intensities are notoriously difficult to obtain for X-ray scattering. The use of calibration samples with small angle X-rays would facilitate calibration of the electron density axis. However, even then, we would still be measuring electron density differences. Absolute measurements of the water content and starch density of the different regions within the granule are possible if the scattering densities of the absorbed water can be varied. This is possible by using small-angle neutron scattering to study starch samples into which mixtures of H_2O and D_2O have been absorbed. In this present paper, the use of SANS to obtain quantitative determination of the water content in the different regions of waxy maize starch granules is described.

Neutron scattering experiments study differences in scattering length, where the scattering length depends on the scattering nucleus. Different isotopes have different scattering length densities, and in particular hydrogen and deuterium have very different neutron scattering lengths. Herein lies the advantage of changing the H_2O : D_2O ratio, so that we can obtain a range of scattering length densities. Applying the model-fitting techniques already developed for SAXS experiments, but using water of varying scattering length density, allows a study to be made of how the scattering length density differences between different regions of the granule vary with the scattering length density of the absorbed water. Coupled with a knowledge of the scattering lengths for all of the components in the system, this enables the composition of the three different starch regions to be investigated. For each region we can therefore estimate both the starch : water ratio and the starch density.

Only one previous study has used small-angle neutron scattering to study starch granule structure. Blanshard *et al.*[3] examined starch samples from various botanical sources in mixtures of H_2O and D_2O. For each sample in pure D_2O a small angle peak was observed. The repeat distance associated with this peak was determined by simple Bragg peak analysis of the peak position, thus resulting in the measurement of a range of repeat distances for the different samples. For potato starch, this study demonstrated that an appropriate mixture of H_2O and D_2O could be used to contrast-match the scattering length densities of the crystalline and amorphous lamellae, thereby causing the small-angle peak to disappear. However, more detailed information about the structure and composition of the different regions within the granule was not obtained.

EXPERIMENTAL

Neutron scattering

Small-angle neutron scattering experiments were carried out on the LOQ station at the ISIS spallation neutron source, Rutherford Appleton Laboratory, UK. The native structure of waxy maize starch, a gift from National Starch and Chemical, Manchester, UK, was examined. The starch samples were in the form of slurries in mixtures of H_2O and D_2O. Samples of water with the required molar ratio of H_2O to D_2O were prepared first, and these were then added to vacuum dried starch to form 45 wt% starch slurries. In order to ensure complete exchange, the samples were left to stand for 24 h, the starch was filtered off, dried in a vacuum oven, and then re-slurried in the same concentration with more water of the same molar ratio of H_2O to D_2O. A standing time of 24 h was chosen, by reference to infra-red spectroscopic studies that have shown that hydrogen–deuterium exchange in starch reaches an equilibrium after 24 h[15]. The slurries

were mixed in 1 mm pathlength quartz cells obtained from Helma (part number 6100, blue). Quartz cells are used since they are transparent to neutron beams. The neutrons scattered from the sample cell were detected by a ^{3}He detector situated 4.4 m distant from the sample. The neutron beam was collimated to a size of 8 mm diameter at the sample.

Data collection

Waxy maize starch was studied as a 45 wt% slurry with eight different mixtures of H_2O and D_2O. On a molar basis, the H_2O contents were 100, 90, 80. 60, 40, 20, 10, and 0%. Measurements were made of the scattered intensity, monitor count and transmission for the eight samples, for an empty cell, and for the mixture H_2O and D_2O (known as background scattering). The collection times for the scattered intensity measurements were all 45 min, while the collection times for the transmission measurements were all 5 min. Data were corrected to allow for detector efficiency, and fully calibrated values of the differential cross section $\partial\sigma/\partial\Omega$ were obtained for the sample, for the empty cell and for the background. The data were rebinned in terms of the scattering vector q, the empty cell scattering was subtracted from the sample and the background data, and the data then radially averaged. The incoherent scattering was removed by subtracting a weighted sum of the pure H_2O and pure D_2O backgrounds. The weighting factor was selected in order to set the intensity at high q equal to zero.

After applying these corrections we have eight data sets of differential scattering cross-section against q. These data sets are calibrated so that the scattering cross-sections have units of cm^{-1}. The calibration was checked by using the scattering from a calibrant sample of known scattering cross-section.

Evaluating the local scattering length densities

For starch immersed in a mixture of H_2O and D_2O some exchange may take place between the hydrogen atoms in the starch and the deuterium atoms in the water. It is known that three hydrogen atoms within the starch molecule are free to exchange[3]. Assuming that the fraction of exchanged starch molecules is the same as the fraction of D_2O present we can determine the scattering length density for starch as follows:

$$\begin{aligned}\bar{b}_{\text{starch}} &= \frac{b_{C_6H_{10}O_5}}{M_{v(C_6H_{10}O_5)}}x \\ &+ \frac{b_{c_6H_7D_3O_5}}{M_{\nu(C_6H_7D_3O_5)}}(1-x) \\ &= \frac{N_A\rho_{\text{starch}}b_{C_6H_{10}O_5}}{162}x \\ &+ \frac{N_A\rho_{\text{starch}}b_{c_6H_7D_3O_5}}{165}(1-x) \qquad (4)\end{aligned}$$

where x is the molar fraction of H_2O and M_v is the molar volume.

Our model for the starch granule structure (detailed in *Figure 1*) includes three different regions, i.e. amorphous lamellae, crystalline lamellae, and an amorphous background. Each region might be expected to absorb a different fraction of water. Furthermore, since the starch structure is likely to be different in each region, so too is the starch density. For each region, we consequently have a different scattering length density, defined as follows:

$$\bar{b}_b = f_b\bar{b}_{\text{water}} + (1-f_b)\bar{b}_{\text{starch(b)}} \qquad (5a)$$

$$\bar{a}_b = f_a\bar{b}_{\text{water}} + (1-f_a)\bar{b}_{\text{starch(a)}} \qquad (5b)$$

$$\bar{b}_c = f_c\bar{b}_{\text{water}} + (1-f_c)\bar{b}_{\text{starch(c)}} \qquad (5c)$$

where $\bar{b}_b$, $\bar{b}_a$, and $\bar{b}_c$ are the scattering length densities for the amorphous background, amorphous lamellae and crystalline lamellae, respectively; f_b, f_a and f_c are the volume fractions of water in the amorphous background, amorphous lamellae and crystalline lamellae, respectively, and $\bar{b}_{\text{water}}$ is evaluated from the particular percentage of D_2O.

When the model developed for SAXS is applied to small-angle neutron data, it will provide values for the scattering length density differences, $\Delta\rho$ and $\Delta\rho_u$, where:

$$\Delta\rho = \bar{b}_c - \bar{b}_a \qquad (6a)$$

$$\Delta_{\rho u} = \bar{b}_b - \bar{b}_a \qquad (6b)$$

However, absolute values of $\Delta\rho$ and $\Delta\rho_u$ will only be obtained if the scattered intensity predicted by the model function can be exactly mapped on to the measured differential cross-section, $\partial\sigma/\partial\Omega$. This requires a knowledge of the number density of the lamellar stacks. Unfortunately, this quantity is not known for starch, and consequently an exact mapping between the predicted and measured scattered intensity is not possible. We must introduce a constant K into the above equations (6), where:

$$\Delta\rho = K(\bar{b}_c - \bar{b}_a) \qquad (7a)$$

$$\Delta\rho_u = K(\bar{b}_b - \bar{b}_a) \qquad (7a)$$

These equations depend only on the values of f_c, f_a, ρ_c, ρ_a, ρ_b, x and K. By varying the value of x, we can obtain a set of pairs of equations (7) to solve simultaneously in order to generate values for f_b, f_a, f_c, ρ_c, ρ_a, ρ_b, and K. A knowledge of f_b, f_a, f_c, ρ_c, ρ_a, and ρ_b tells us much about the composition of the different regions within the starch granule. Since we have seven unknown variables, and

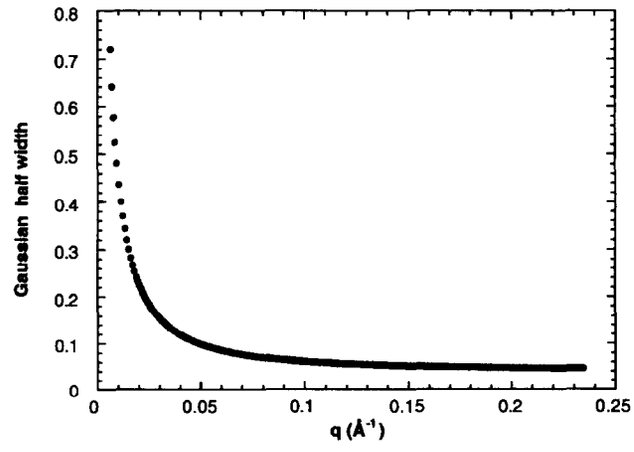

Figure 2 The neutron resolution function used for convolution, with the data, plotted as the full width at half maximum of a Gaussian distribution, as a function of q

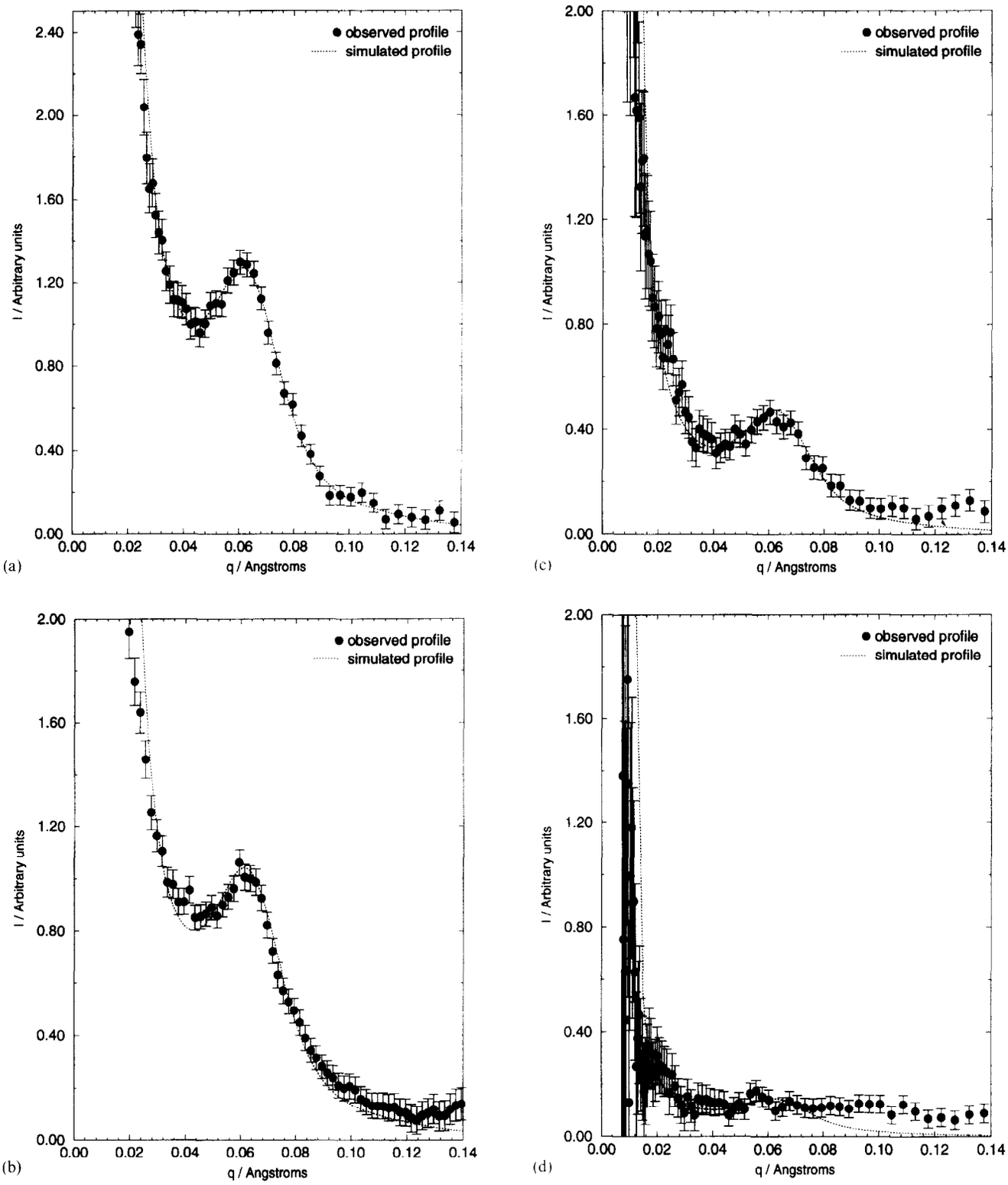

Figure 3 Comparison of observed and simulated scattering profiles for 45 wt% waxy maize starch slurries in: (a) 100% H_2O; (b) 90% H_2O, 10% D_2O; (c) 80% H_2O, 20% D_2O; (d) 60% H_2O, 40% D_2O; (e) 40% H_2O, 60% D_2O; (f) 20% H_2O, 80% D_2O; (g) 10% H_2O, 90% D_2O; (h) 100% D_2O

each value of x generates two equations, we need at least four values of x to evaluate values for the seven variables.

Fitting the SANS profile to measure structural parameters

The expression previously derived to predict the small-angle X-ray scattering from a model starch granule structure[4] is equally applicable to small-angle neutron scattering. Therefore, the same fitting routines can be applied to obtain structural information from the small-angle scattering profile. However, in the case of neutrons we will measure scattering length density differences, rather than electron density differences.

As discussed in the previous section, it is not possible to map exactly the predicted scattering from the model function on to the measured scattering cross section, $\partial\sigma/\partial\Omega$. An arbitrary constant must be introduced. This constant will depend on the sample volume, the number

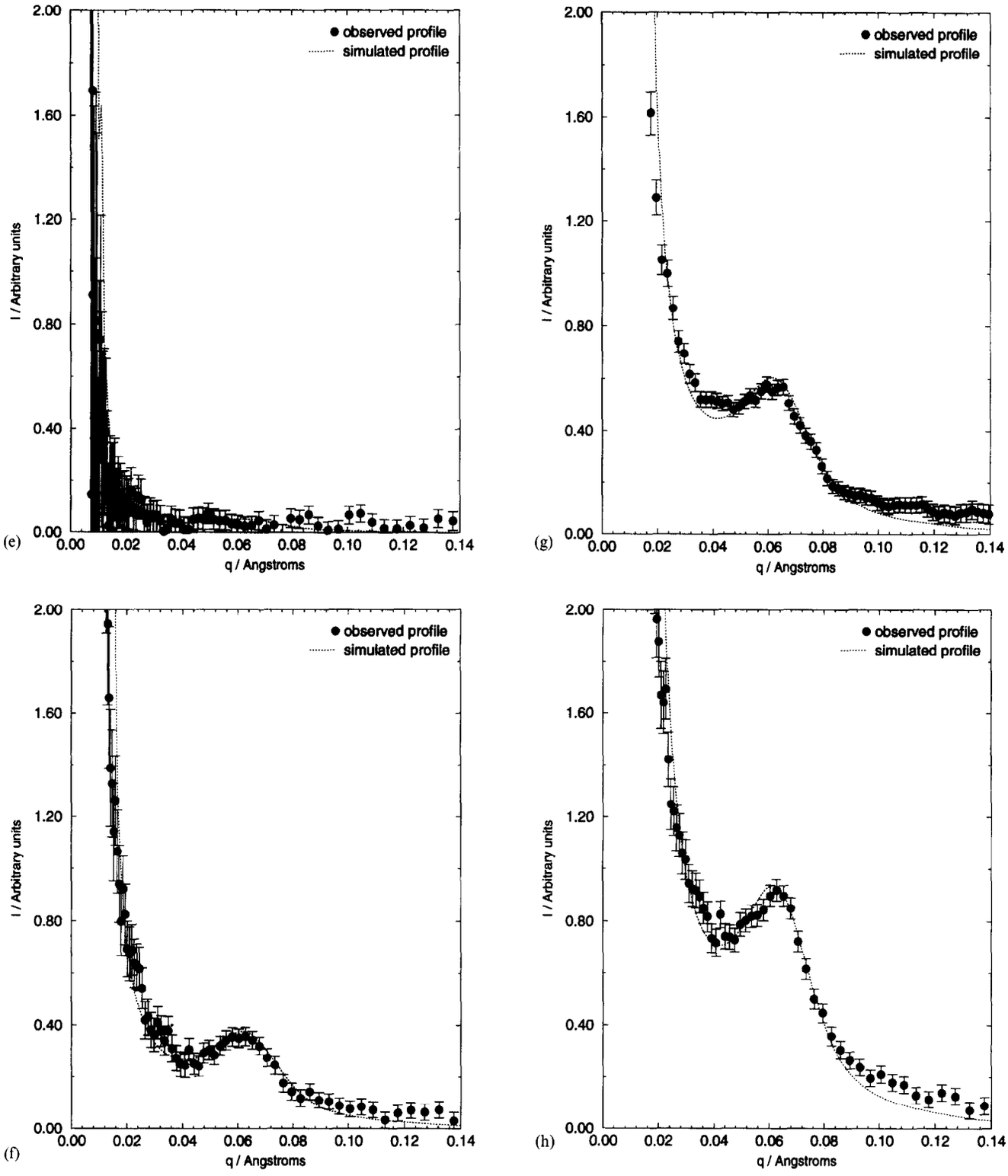

Figure 3 *(Continued)*

density of scattering objects and a geometrical term. The introduction of this arbitrary constant also means that absolute values of scattering length density differences cannot be measured. All values are instead plotted on the same relative scale. Seen in this way, the SANS results are no improvement on simply using SAXS analysis. However, the key advantage of using SANS is the ability to vary the scattering density of the absorbed water, which enables us to determine compositional information for each of the three regions within the granule. Such information is inaccessible by SAXS studies where the analogy of changing the contrast of the water does not exist.

With two modifications the scattering profiles were fitted in the same manner as described in earlier papers for SAXS[4,14,16]. The first modification was to include the resolution correction. The resolution function used is shown in *Figure 2*. This was calculated by using a program written by Dr Adrian Rennie, University of Cambridge. The second modification is a change in the least-squares fitting algorithm to take account of the error bars on the neutron-scattering data points. This is

Table 1 Comparison of fitting parameters of 45 wt% waxy maize starch in 100% H_2O when studied by SANS and SAXS

Scattering probe	d (Å)	N	ϕ	β	$\Delta\rho$	$\Delta\rho_u$
Neutrons	89	24	0.69	0.35	2.42	−0.20
X-rays	88	20	0.67	0.36	1.36	0.92

not necessary for the equivalent X-ray data, since the error on each point was extremely small.

By applying the corrections described above, each SANS profile may be fitted to yield values for the six structural parameters of the model: the number of lamellae in the stack (N), the average repeat distance between the crystalline lamellae (d), the fraction of this repeat distance that is crystalline (ϕ), a parameter defining the distribution of lamellar sizes (β), and two scattering length density differences, i.e. between the crystalline and amorphous lamellae ($\Delta\rho$), and between the amorphous lamellae and amorphous background ($\Delta\rho_u$). Further details of the model are provided in ref. 4. An investigation of the changes in $\Delta\rho$ and $\Delta\rho_u$ as the scattering length density of the absorbed water is varied provides compositional information about the amorphous lamellae, crystalline lamellae and amorphous background.

Elucidating compositional information

Fitting of each of the eight waxy maize SANS profiles provides eight pairs of equations for $\Delta\rho$ and $\Delta\rho_u$—each pair for a different ratio of H_2O to D_2O. Since the various parameters are not known exactly, there will be no exact solution to the simultaneous equations. Instead, what we are looking for here is the best solution, i.e. by finding the solution which minimizes the errors between the fitted solution and the actual equation for all of the eight equations. This was solved by using a 'Mathematica' program. This approach allows upper and lower bounds, and 'best-guess' values to be entered for the variables. The variables, f_b, f_a, and f_c, are all set to range between 0 (all starch) and 1 (all water), with a best-guess value of 0.5. The variables, ρ_c, ρ_a, and ρ_b all have a best-guess value of 1.61 g cm^{-3} (since the partial specific volume of amylopectin[3] is known to be 0.62 cm^3 g^{-1}). Since the value of K is unknown, its value is unconstrained within the minimization routine, and the effect of picking a range of different best-guess values was explored. The values of the variables, f_b, f_a, f_c, ρ_c, ρ_a, and ρ_b, which yield this minimization are assumed to describe the composition of the amorphous lamellae, crystalline lamellae and amorphous background.

RESULTS

Fully corrected plots of $\partial\sigma/\partial\Omega$ vs. q for 45 wt% waxy maize starch in eight different H_2O and D_2O mixtures are shown in *Figures 3a–h*. For each profile, the best-fit simulated profiles (obtained as described below) for a model structure with variable parameters are also shown. The first stage in obtaining these fits consisted in fitting the scattering for 45 wt% waxy maize in 100% H_2O by varying all six structural parameters simultaneously. The structural parameters elucidated from this fit are shown in *Table 1*. This table also records the best-fit structural parameters obtained from model fitting to the SAXS profile from the same sample: values for $\Delta\rho$ and $\Delta\rho_u$ from the two techniques are not comparable, since they are relative to different arbitrary scales. Errors for the structural parameters detailed in *Table 1* are not available, since only a single complete set of data have been collected. When considering the relative accuracies of the recorded scattering profiles (in particular, the SANS profiles recorded around the contrast match point, i.e. *Figures 3d* and *3e*), it is likely that the error on all of the structural parameters measured by analysis of the SANS profiles is much larger than that recorded for the same parameter measured from the SAXS profiles.

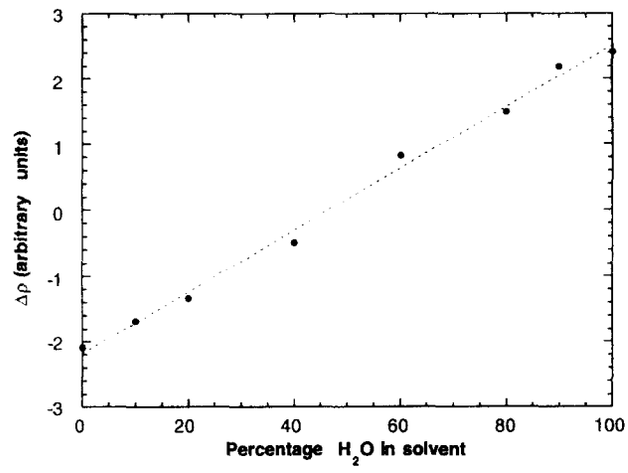

Figure 4 Changes in the value of $\Delta\rho$ as the content of H_2O in the 45 wt% waxy maize slurry in water is varied; assuming that $\Delta\rho$ for 100% H_2O is positive, all other values of $\Delta\rho$ are given either a positive or a negative sign in order to produce a straight-line graph. The dotted line represents the best-fit straight line to these points

In order to fit the other seven 45 wt% waxy maize SANS profiles, it was found necessary to vary only the values of the parameters $\Delta\rho$ and $\Delta\rho_u$. Some thought needs to be given to their sign, since the fitted function has the same value when $\Delta\rho$ and $\Delta\rho_u$ are both negative as when they are positive, and the assignment of the sign to them both is arbitrary. Since the scattering length density for H_2O is negative, while the scattering length density for D_2O is large and positive, it is likely that $\Delta\rho$ is positive for 45 wt% waxy maize starch in 100% H_2O. Making this assumption, *Figure 4* plots out the other values of $\Delta\rho$ so as to obtain a linear change in $\Delta\rho$ with percentage H_2O in the solvent. The best-fit straight line to this plot has an H_2O content of 47 mol% when $\Delta\rho = 0$. This corresponds to a D_2O content of 59 wt%. At this contrast match point the scattering length densities of amorphous and crystalline lamellae are exactly the same.

Figure 5 shows the scattering length density profiles for all of the 45 wt% waxy maize starch slurries (measured values). These plots assume that $\Delta\rho$ is positive for H_2O contents greater than that of the contrast match point, and that this parameter is negative for H_2O contents less than that of the contrast match point.

Taking the values of $\Delta\rho$ and $\Delta\rho_u$ as a function of H_2O content and applying the analysis described previously, we can obtain values for the water contents and starch densities of the amorphous lamellae, crystalline lamellae and amorphous background. However, a unique solution which minimizes the errors is not found,

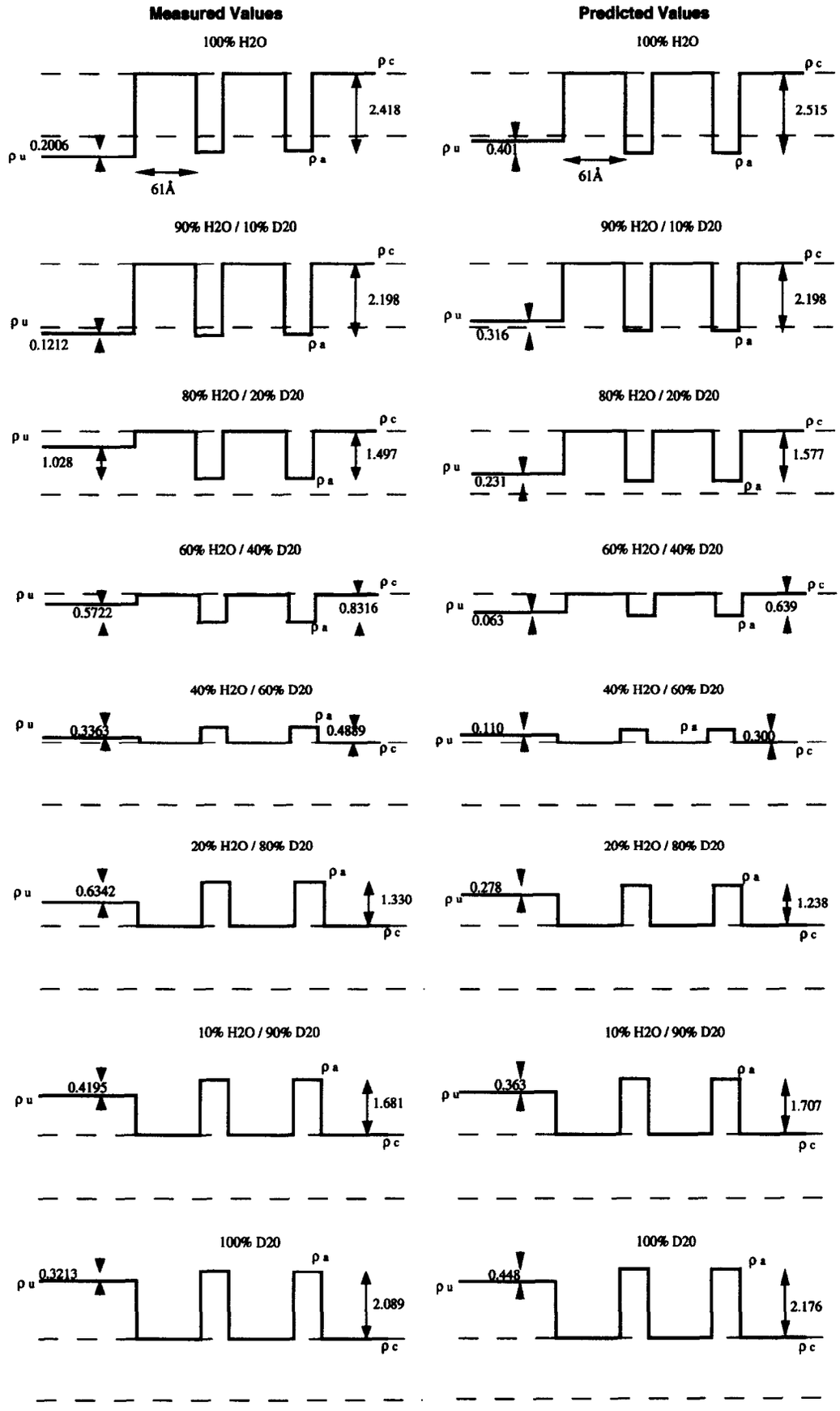

Figure 5 Scattering length density profiles for 45 wt% waxy maize starch as a function of the H_2O and D_2O content of the solvent; measured values are shown on the left of the figure, with the corresponding predicted values on the right

Table 2 Values obtained for the water contents and starch densities within a 45 wt% waxy maize starch slurry in water[a]

Variable	f_b	f_a	f_c	ρ_b ($g\,cm^{-3}$)	ρ_a ($g\,cm^{-3}$)	ρ_c ($g\,cm^{-3}$)	K^b
Value	0.64	0.75	0.11	1.59	1.59	1.72	0.15

[a] a, amorphous lamellae; b, amorphous background; c, crystalline lamellae. Water contents are expressed as volume fractions
[b] Arbitrary fitting constant

with more than one set of values of f_b, f_a, f_c, ρ_c, ρ_a, ρ_b, and K which yield the same minimum value being obtained. Which set of solutions is found by the minimization routine depends upon the initial best-guess value for K. The work of Nara *et al.*[15] and Khairy *et al.*[17] on the accessibility of starch to deuteration suggests that the crystalline region is relatively impenetrable to water. Of the solutions available, that which has the lowest volume fraction of water in the crystalline lamellae was chosen. Having selected this solution, the value of the parameter K is then fixed. The values of all of the variable parameters obtained in this way are detailed in *Table 2*. Since we do not know the error on the values of $\Delta\rho$ and $\Delta\rho_u$ used to calculate the values shown in *Table 1*, it is not possible to quote errors on the values of f_b, f_a, f_c, ρ_c, ρ_a, or ρ_b.

The precise values quoted in *Table 2* may be incorrect. As discussed above, the problem of multiple solutions has required an additional assumption (concerning the water content of the crystalline lamellae) to be made before these values can be obtained. However, all values of K generated values for f_b, f_a, f_c, ρ_c, ρ_a, and ρ_b, that ranked in the same order. Specifically, $f_a > f_b > f_c$, and $\rho_c > \rho_a \sim \rho_b$. These rankings are therefore believed to be correct. Furthermore, having fixed the value of the parameter K, any changes in the values of the variables f_b, f_a, f_c, ρ_c, ρ_a, and ρ_b (e.g. during gelatinization) will be measured exactly. Such a procedure will be described in a subsequent paper, together with alternative methods for constraining K.

By taking the values quoted in *Table 2* it is possible to use the equations described previously to obtain values for $\Delta\rho$ and $\Delta\rho_u$ as a function of the H_2O and D_2O content. These predicted values are used to generate the scattering length density profiles shown in *Figure 5* (predicted values). Comparing these profiles with the experimentally derived profiles detailed in the same diagram provides a test of the accuracy of the minimization technique, and the values of f_b, f_a, f_c, ρ_c, ρ_a, and ρ_b that are generated.

DISCUSSION

The structural parameters obtained from SANS and SAXS investigations of a 45 wt% waxy maize starch slurry in 100% H_2O are listed in *Table 1*. Apart from the values of $\Delta\rho$ and $\Delta\rho_u$—for which consistency has no meaning since they are in different units—all other structural parameters are highly consistent. As expected, our structural analysis technique is not influenced by the scattering probe, and is equally applicable to both SANS and SAXS studies.

Figure 5 describes the changes in scattering length density profile recorded as a function of H_2O and D_2O content (measured values). As expected, replacing hydrogen by deuterium does not change any of the structural parameters apart from $\Delta\rho$ and $\Delta\rho_u$. For both 100% H_2O and 100% D_2O we observe a large difference in the scattering length density difference between the crystalline and amorphous lamellae ($\Delta\rho$). This is expected from the intense SANS peaks observed for these samples (*Figures 3a* and *3h*). For waxy maize starch in other mixtures of H_2O and D_2O, $\Delta\rho$ was smaller in magnitude. The point at which $\Delta\rho = 0$ was measured to occur when the content of D_2O was 59 wt%. An earlier study measured this contrast match point to be 52 wt% D_2O for potato starch[3]. Since this other study employed a different technique to locate the contrast match point, and because the errors in measuring this point are large, it is not possible to conclude whether the difference in the values recorded for these two different starches is significant.

By using the measured values of $\Delta\rho$ and $\Delta\rho_u$ as a function of the H_2O and D_2O content it is possible to determine the fractional water contents and molecular starch densities for the three regions within the starch granule. These values are recorded in *Table 2*. In order to assess the accuracy of these values, the values of $\Delta\rho$ and $\Delta\rho_u$ that they predict were recorded, and used to construct predicted scattering length density profiles. These predicted profiles are shown in *Figure 5* (predicted values). Visually, these profiles agree very well with the measured profiles shown in the same diagram. In particular, we observe a very good correlation between the measured and predicted values of $\Delta\rho$. The correlation between the measured and predicted values of $\Delta\rho_u$ is less good. However, it is known from the X-ray scattering experiments that values of $\Delta\rho_u$ are inherently less accurate than values of $\Delta\rho$[14]. Furthermore, the large errors associated with the SANS profiles will result in a larger error in the values of $\Delta\rho$ and $\Delta\rho_u$ when compared with the X-ray results. The errors in the values of $\Delta\rho$ and $\Delta\rho_u$ obtained from SAXS analysis have been estimated to be ± 0.05 and ± 0.1, respectively[18]. The exact errors for $\Delta\rho$ and $\Delta\rho_u$ measured from the SANS profiles are not available, but are expected to be significantly larger than this. When comparing the measured and predicted scattering length density profiles, the largest differences between the predicted and measured values are found to be 0.2 for $\Delta\rho$ and 0.8 for $\Delta\rho_u$. Considering the relative accuracies of the recorded scattering profiles (in particular, the SANS profiles recorded around the contrast match point, i.e. *Figures 3d* and *3e*) it is likely that the error on $\Delta\rho$ and $\Delta\rho_u$ measured from the SANS profiles is large enough to explain these differences. We may therefore conclude that the minimization routine gen-

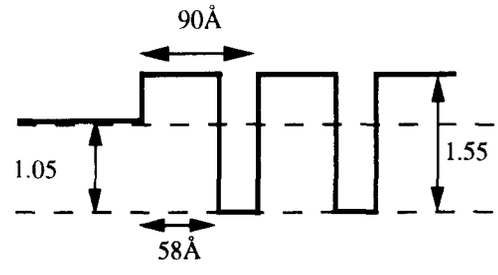

Figure 6 Electron density profile for waxy maize starch based on SAXS data (after ref. 19)

erates reasonable values for the parameters f_b, f_a, f_c, ρ_c, ρ_a, and ρ_b.

The results shown in *Table 2* suggest very large volume fractions of water are present within the amorphous regions of the granules. They also suggest that more water is present within the amorphous lamellae than within the amorphous background region. This observation is consistent with previously published SAXS investigations of the structure[19]. The electron density profile recorded for waxy maize starch (*Figure 6*) has a significantly greater electron density within the amorphous background than within the amorphous lamellae. As it has a lower density than starch, water has a lower electron density. Assuming that all other variables remain constant, an increased volume fraction of water within a specific region will consequently lower the electron density of that region. That more water penetrates the amorphous lamellae than the amorphous growth ring suggests that the amorphous lamellae has a more open structure than the amorphous growth ring. This is not surprising. The amorphous lamellae are composed primarily of amylopectin branch points. Steric packing problems are therefore likely to produce a more open structure within the amorphous lamellae than within the amorphous growth ring.

The ease of water penetration into the amorphous lamellae is likely to be accentuated for waxy maize starch due to the relatively large size of the amorphous lamellae in this type of starch when compared with other starch samples: the amorphous lamellae in waxy maize starch have been measured to be 32 Å thick (*Figure 6*), compared to a thickness of 23 Å for normal maize[19]. Thus the conclusion reached here of more water being contained within the amorphous lamellae than within the amorphous growth ring for waxy maize starch need not necessarily be true for other starch species.

As discussed above, the water content for the crystalline region recorded in *Table 2* was taken to be very low, in order to allow a unique choice to be made between the different sets of solutions. This minimum value is selected to agree with the results of other studies[15,17].

The starch molecular densities recorded in *Table 2* are observed to be very similar within the two types of amorphous regions of the granule, but are higher within the crystalline lamellae. In all cases, these densities differ very little from the known molecular density of amylopectin. Any large deviation in the molecular density measured by using the SANS technique from the density previously measured for amylopectin would indicate a different structure for amylopectin within the granule and amylopectin outside the granule. Since we do not observe any such large deviation we may conclude that the amylopectin structures observed outside the granule are likely to be valid representations of the structures found inside the granule. This finding is consistent with all other experimental studies such as those based on wide-angle X-ray scattering (WAXS) studies[20–26] or nuclear magnetic resonance (n.m.r.) spectroscopic studies.

CONCLUSIONS

The use of small-angle neutron scattering to study the structure of starch granules has provided a new insight which supplements that obtained by recent SAXS studies. The independent application of the model fitting technique to the SANS profile for waxy maize starch in 100% H_2O has provided a test of this method for obtaining structural information. The close agreement observed between the structural parameters measured from the SANS profiles with those obtained from the SAXS profiles confirms both the values of these parameters, and provides clear evidence that fitting our theoretical function derived for a model structure to small-angle data is a robust analytical technique.

As found in a previous SANS study on potato starch[3], this investigation has revealed that a particular mix of H_2O and D_2O will contrast-match the scattering densities of the amorphous and crystalline lamellae. When studied in this mix of H_2O and D_2O the SANS profile is very weak. The contrast-match point for waxy maize starch was found to be similar to that measured earlier for potato starch[3].

As expected, it has proved possible to fit the SANS profiles for waxy maize starch in all mixtures of H_2O and D_2O by varying only the scattering length densities in the model scattering function. Varying the mixture of H_2O and D_2O does not therefore affect the structural dimensions within the granules. By using the results obtained for the variation in $\Delta\rho$ and $\Delta\rho_u$ with H_2O and D_2O content, we are able to determine values for the water content and starch density within the amorphous lamellae, crystalline lamellae, and the amorphous background regions. Although the value for these parameters quoted in this study may not be precisely correct, their relative magnitudes suggest a large volume of water to be present at room temperature within the amorphous lamellae, slightly less within the amorphous background, and very little within the crystalline lamellae. The molecular density of the starch is greatest within the crystalline lamellae, but in all of the cases it does not differ much from the recorded molecular density of amylopectin. Scattering length density profiles calculated by using the values for water content and molecular starch density for the three regions are consistent with the experimentally measured scattering profiles.

Based on this preliminary study of the native structure of the waxy maize starch, we have confirmed the usefulness of this technique for starch studies. A subsequent paper will extend the methodology to consider what happens to the water content in the different regions of the granule during gelatinization, which it is hoped will provide new information on the gelatinization mechanism.

ACKNOWLEDGEMENTS

Thanks are due to Professor Randal Richards of Durham University, who first suggested that SANS would be a useful approach to complement SAXS, to Dr J. Penfold at the Rutherford Appleton Laboratory, and to Tom Waigh and Dr A. Rennie for many useful discussions and help with the data analysis. The financial support of the BBSRC and Dalgety PLC through a cooperative studentship to P.J.J. is gratefully acknowledged.

REFERENCES

1 French, D. in 'Starch: Chemistry and Technology' (Eds R. L. Whistler, J. N. BeMiller and E. F. Paschall), Academic, London, 1984, p. 183

2 Sterling, C. J. *Polym Sci.* 1962, **56**, S10
3 Blanshard, J. M. V., Bates, D. R., Muhr, A. H., Worcester, D. L. and Higgins, J. S. *Carbohydr. Polym.* 1984, **4**, 427
4 Cameron, R. E. and Donald, A. M. *Polymer* 1992, **33**, 2628
5 Kassenbeck, V. P. *Stärke* 1975, **27**, 217
6 Kassenbeck, V. P. *Stärke* 1978, **30**, 40
7 Oostergetel, G. T. and Bruggen, E. F. J. V. *Carbohydr. Polym.* 1993, **21**, 7
8 Oostergetel, G. T. and Bruggen, E. F. G. V. *Stärke* 1989, **41**, 331
9 Robin, J., Mercier, C., Charbonniere, R. and Guilbot, A. *Cereal Chem.* 1974, **51**, 389
10 Robin, J. P., Mercier, C., Duprat, F., Charbonnière, R. and Guilbot, A. *Stärke* 1975, **27**, 36
11 Jenkins, P., Cameron, R. E. and Donald, A. M. *Stärke* 1993, **45**, 417
12 Matsuo, M., Sawatari, C., Tsusi, M. and Manley, R. S. J. *J. Chem. Soc. Faraday Trans.* 1983, **79**, 1593
13 Hosemann, R. *Z. Phys.* 1949, **127**, 16
14 Cameron, R. E. and Donald, A. M. *Carbohydr. Res.* 1993, **244**, 225
15 Nara, S., Takeo, H. and Komiya, T. *Stärke* 1981, **33**, 329
16 Cameron, R. E. and Donald, A. M. *J. Polym. Sci. Polym. Phys. Edn.* 1993, **31**, 1197
17 Khairy, M., Morsi, M. and Sterling, C. *Carbohydr. Res.* 1966, **3**, 97
18 Jenkins, P. J. *PhD Thesis*, Cambridge University, 1995
19 Jenkins, P. J. and Donald, A. *Int. J. Biol. Macromol.* 1995, **17**, 315
20 Wu, H. and Sarko, A. *Carbohydr. Res.* 1978, **61**, 7
21 Wu, H. *Carbohydr. Res.* 1978, **61**, 27
22 Imberty, A., Chanzy, H., Pérez, S., Buléon, A. and Tran, V. *Macromolecules* 1987, **20**, 2634
23 Imberty, A. and Pérez, S. *Biopolymers* 1988, **27**, 1205
24 Imberty, A., Chanzy, H., Pérez, S., Buléon, A. and Tran, V. *J. Mol. Biol.* 1988, **201**, 365
25 Imberty, A. and Pérez, S. *Int. J. Biol. Macromol.* 1989, **11**, 177
26 Imberty, A., Buléon, A., Tran, V. and Pérez, S. *Starch* 1991, **43**, 375
27 Gidley, M. J. and Bociek, S. M. *J. Am. Chem. Soc.* 1985, **107**, 7040